Contents

Chapter 1

Shape and dynamics

When it's seen by naked eye, plasma sources for medical uses expel a little plume of plasma that emits radiation in a visible range, with different colours or intensity that depends on the gas composition, it's flow and intensity of applied electric field. However if we see this plasma at a specific time, recent studies shows that what is expelled is not a continuos flow, but the "plume" is formed by compact bullets with high velocities ([6], [8]). An example of this phenomenon is shown in figure 1.1, measured with the experimental apparatus that will be explained later.

Plasma bullets still needs to be studied in depth, we only know the basic dynamic of formation and expulsion. Some general features are that:

- bullet's velocities are $> 10\,\mathrm{km/s}$;
- bullet formation, it's velocity and it's travel distance depend on applied tension on the electrode;
- frontal image of the bullet, on a plane perpendicular to it's velocity, is not a full circle but it's donut shaped, with an outer ring of higher intensity.

The scope of this experiment is to observe plasma bullets produced with our source, their shape and their velocity and how they change with different discharge conditions.

Given their typical velocities and the temperature of the plasma, bullet propagation is tought to be related to a travelling ionization front. This propagation can be studied with simplified simulation of DBD discharges, where it's reproduced the behavior of plasma bullets ([10], [3]) or the interaction between plasma and a target ([7]).

1.1 Experimental setup

To visually observe dynamics of plasma formation and propagation, it is needed an acquisition setup with an high-speed camera that has little integration time, around $10\,\mathrm{ns}$, and an image intensifier that permits to visualize light emitted in such a short time interval.

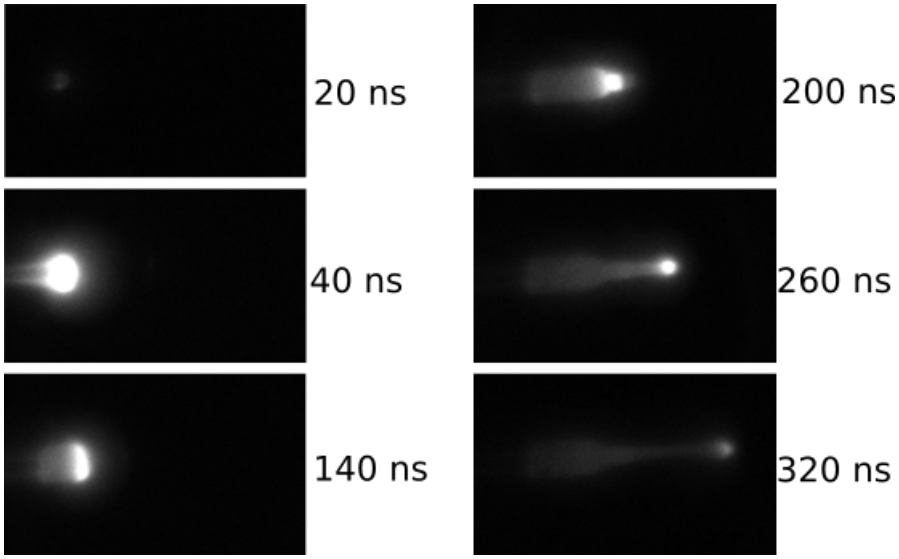

Figure 1.1: Example of plasma bullet expulsion, as measured with our experimental setup, with an helium flow of 2 L/min.

This is a measure where we need coincidence between discharge and frame measure so it is necessary to consider instruments and plasma source specific delays and give appropriate triggers.

Experimental setup is shown in photo 1.2 and a scheme is presented in 1.3, there are the trigger signal lines, optical acquisition pointed at source exit and measure acquisition composed by a computer and an oscilloscope.

1.1.1 Source and optical setup

Source head is positioned vertically and emitted light is collected from the side. Optical apparatus is composed by a lens coupled with a Micro Channel Plate image intensifier (MCP). An MCP works as in figure 1.4: for every photon received, thanks to an high-voltage power supply, it emits many photons with little angular deviation.

Those photons are received by an high-speed camera *Point Grey Flea* ([1]) equipped with a CCD of 1024×768 square pixels 4.75 µm wide. Every frame is sent to the pc where FLIR software elaborates and saves them in pgm format ([2]).

1.1.2 Source, power lines and electric signals

It's used a source with electric features and functioning similar to those described before, with an output between 3 and 8 kV, variabile changing Δt of the trigger signal (see **??**), that is always given through an optical fiber with frequency f. Differances are that tension is positive and not negative, because it helps formation of the plume with gasses harder to ignite (e.g. Argon), and that trigger signal is given by a generator function (2 in the scheme) to define discharge time respect to the trigger of other instruments.

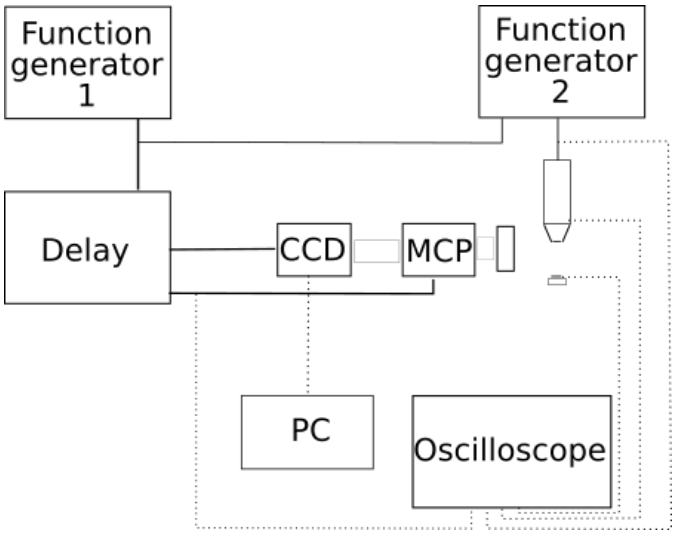

Figure 1.2: Photo of the experimental setup.

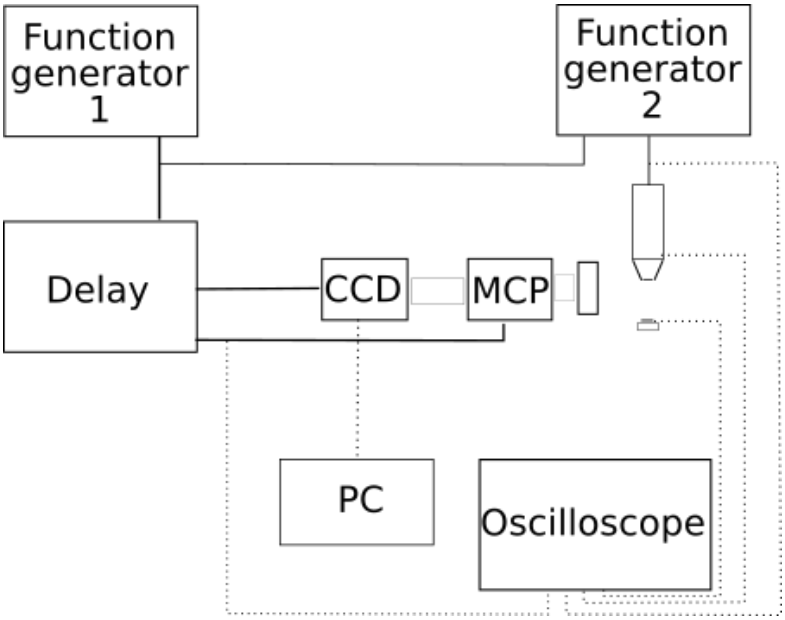

Figure 1.3: Experimental setup scheme. Function generator 1, function generator 2 and delay generator send trigger signal to camera (CCD), to source and to image intensifier (MCP), full lines in the scheme. Camera sends measured frame to a computer (PC) and from source, source's target, function generator 2 and delay are taken signals read on the oscilloscope, pointed lines in the scheme.

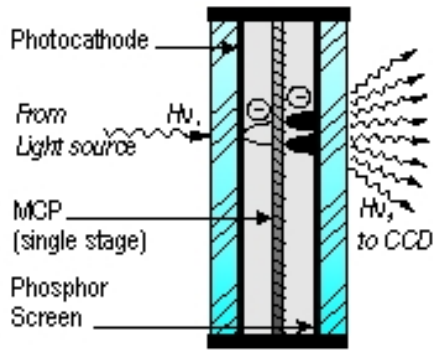

Figure 1.4: Micro Channel Plate image intensifier functioning.

The source is positioned vertically at a distance of 42.0 ± 0.1 mm from optical bench, with the glass nozzle that permits to observe plasma formation inside it (external diameter 8.0 ± 0.1 mm, internal diameter 6.0 ± 0.1 mm), with a distance from the end of the electrode to nozzle exit of 12 mm. At the exit the nozzle shrinks for 3.0 ± 0.1 mm, until a diameter of 5.0 ± 0.1 mm

Under the source is possible to put targets. Are used two different targets at different heights: conductive target and insulator target. The first one is a copper square sheet of dimensions $10\,\text{mm} \times 10\,\text{mm} \times 1\,\text{mm}$ (used for current measures in chapter **??**), the second one is a simple plastic material.

CCD camera is powered by a simple alimentator while image intensifier MCP is powered by an high-voltage supply, both are triggered by the delay generator, with different times (see next section).

On an oscilloscope are measured the trigger signal given to source head, the trigger signal given to MPC, the voltage electrode with high-voltage probe *Tektronix P6015A* and the current intensity when it's used the conductive target. Current intensity measure is done measuring voltage drop on a resistance of $1\,\text{M}\Omega$ with a probe $x10$.

1.1.3 Trigger synchronization

Experiment's scope is to know plasma dynamics at a specific point on voltage waveform, so it's necessary to know precisely discharge and measure times.

To compose the necessary trigger line are utilized:

- function generator *Or-x 310*, 1 in figure, that sends a square wave with set amplitude, width and frequency f;
- function generator *Lecroy 9210*, 2 in figure, that sends a square wave with frequency given by the trigger, amplitude set, and variable width Δt;
- delay time generator *Stanford DG535*, that sends square wave with set amplitude, frequency given by the voltage input and starting times given by voltage input

startin time plus settable delays (4 channels).

Every intrument has it's own time that elapse between trigger signal and effective measure. The longer one is arming time for high-speed camera in the order of ms, the smaller one is integration time for acquisition system, that starts from the activation of the image intensifier and span 15 ns.

A time line is shown in figure 1.5, an example of signal taken with the oscilloscope is in figure 1.6. There are three relevant times defined by function and delay generators:

1. t_0 is the starting time for the square wave given by *Function generator 1*, with an amplitude of 5 V and a frequency f, that goes as external trigger to *Function generator 2* and as voltage input to *Delay generator*. From *Function generator 2*, at t_0, starts the square wave that triggers discharge, with a width of Δt that will define voltage amplitude (see chapter **??**) and the same frequency f. From *Delay generator*, at t_0, without delays, starts the trigger signal to arm the camera with the CCD.

2. t_{DIS} is the effective discharge time, when the amplitude peak starts. From trigger signal end to amplitude peak start there is a time delay given mainly by the response time of photodiode. Measuring the signals as in figure 1.6, it's possible to estimate this delay as 987.7 ± 56.7 ns, constant for every f and Δt. Once the discharge starts, in the grey zone in figure, there are the events that we want to measure, plasma formation and propagation.

3. t_{MIS} is the measure time, when the MCP is triggered on. The delay between t_0 and t_{MIS}, t_D, is given by the *Delay generator* with possible steps of 1 ps. Changing t_D during measure it's possible to see plasma dynamics at different times that corresponds to different points on electrode tension waveform, as in figure 1.6.

Integration time for a single frame is 15 ns, so the time step between two measures has to be larger then it. For slow plasma bullets (Neon or Argon) it's used a step of 50 ns, for fast bullets (Helium) it's used a step of 20 ns.

The effective measure time have to consider slower time of the camera, larger then 50 ms. It's important to note that also with little frequencies, around 50 Hz (see later the minimum working frequency for different gasses), time between two pulses is 20 ms, so it is not possible to see two consecutive frames, we observe the same time in different discharges.

Changing the settings on camera acquisition software is possible to measure a signal below pixel's saturation point. One of the parameters is the *Shutter time*, the opening time of the camera shutter, that if set on a value larger then the time between two signals permits to integrate between two frames. When we work with a gas, we select an appropriate *Gain* value and an appropriate *Shutter time*, chosing to work measuring a single discharge frame or a multiple discharge frame.

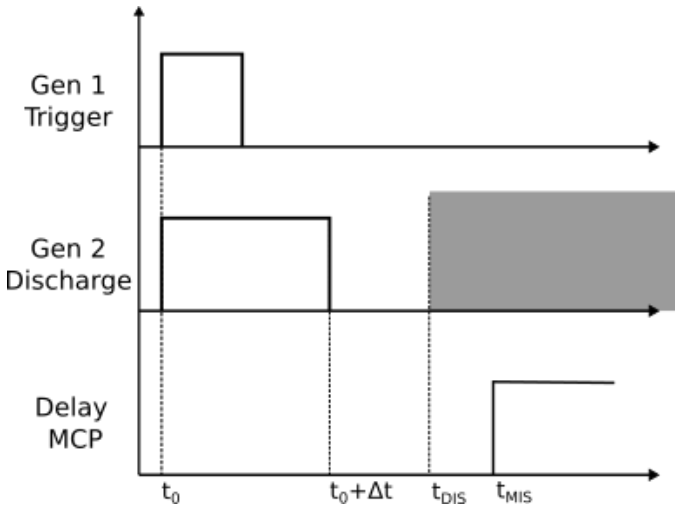

Figure 1.5: Time signal synchronization scheme: t_0 is the starting trigger time, Δt is the opening time for plasma source (see chapter **??**), t_{DIS} is the starting time for the discharge and t_{MIS} the starting time for the MCP i.e. the measure time

.

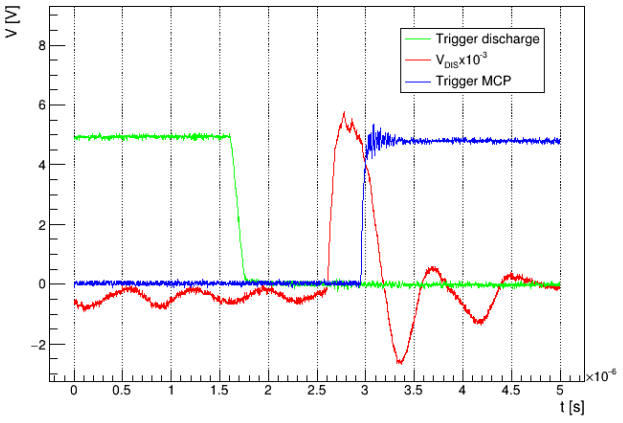

Figure 1.6: Oscilloscope measure example, in green the discharge trigger, in red the electrode tension output and in blue the MCP trigger.

1.1.4 Different setups

Plasma formation is influenced by many parameters such as frequency of high-voltage pulses, their rise time and maximum, gas type, gas flow, presence of a target and its features (see [6], [5]).

For pulse frequency we find a lower limit value, different for each ignition gas, under which there is no discharge. For frequencies higher then this value we don't expect changes (as there aren't in the electric behavior in chapter **??**), so we use a single chosen value that permits plasma ignition and doesn't stress the experimental setup. High-voltage values and gas type determine plasma bullet formation and affect its expulsion velocity. In particular, different gasses have different atomic mass and ionization energies, they will have different voltage ignition values and reactive species formed in plasma will have different velocities. Gas flow influences how much gas there is when the ignition starts, so varying it we observe different bullets diameter and velocity. Target influences bullet expulsion, propagation and plasma rebound signal. With a conductive target near plasma exit we will have an easier path seen by charges that propagates and, once the bullet hits the target, its observed higher luminosity going from the target to the electrode. With an insulator target we don't find the ionization channel closing on the target, but we observe charge deposition on the insulator with a shape that depends from the gas and the target. In some setups, to help plasma ignition it's also used a conductor ring at ground potential or at floating potential, placed around source nozzle, after the electrode position.

In this study we present different setups with three different gasses, as shown in table 1.1.

1.1.5 Frame analysis and calibration

Once a measure setup is chosen, t_D is set around the start of the discharge, we measure the oscilloscope waveform for every channel (setup as explained before), and from them we save 5 frames for every t_D varying it with steps of Δt_D. Measures are taken until the end of the main tension peaks and the camera doesn't see anything.

From oscilloscope waveforms we can extrapolate the measure time from the start of the discharge and tension value at measure time. When there is the conductive target it's also possible to see current intensity and it's peak time.

Frame analysis is done converting the pgm files in 2-dimensional histograms, using *TH2* class written in *ROOT* libraries (see [4]). We are interested in plasma bullet formation and it's expulsion, but also in other fenomenological behavior that is observed during measures.

For plasma bullet we take the mean for every pixel between the five frames taken, from then it's isolated the plasma bullet as the collection of pixels with maximum intensity in the frame. From this image we extrapolate the position of the bullet with the coordinates of it's luminosity barycenter on the plane seen by camera, called x-y in the analysis. Once established the center, we can find it's contour as the points were luminosity goes under a certain percentage of the maximum, from that we estimate it's dimensions along x and

Gas	Setup	Δt	Target	Target distance	Flow rate	Other	Δt_D
He	A	30, 35, 40	Conductor	24 mm	2 L/min	-	50 ns
	B	30, 35, 40	Conductor	32 mm	2 L/min	-	20 ns
	C	30, 35, 40	Insulator	24 mm	2 L/min	-	20 ns
	D	30, 35, 40	-	-	2 L/min	-	20 ns
	E	35	-	-	2 L/min	Ground ring	20 ns
	F	35	-	-	1 L/min	-	20 ns
	G	35	-	-	3 L/min	-	20 ns
	H	35	-	-	4 L/min	-	20 ns
Ne	A	20, 25, 30	Conductor	24 mm	2 L/min	-	50 ns
	B	20, 25, 30	Conductor	32 mm	2 L/min	-	50 ns
	C	20, 25, 30	Insulator	24 mm	2 L/min	-	50 ns
	D	20, 25, 30	-	-	2 L/min	-	50 ns
	E	30	-	-	2 L/min	Ground ring	50 ns
Ar	A	35	-	-	2 L/min	Ground ring	50 ns
	B	35	-	32 mm	2 L/min	-	20 ns
	C	35	-	-	2 L/min	Floating ring	50 ns
	D	35	Conductor	20 mm	2 L/min	Ground ring	50 ns
	E	35	Conductor	20 mm	2 L/min	-	50 ns
	F	35	-	-	2 L/min	-	50 ns
	G	35	Conductor	32 mm	2 L/min	-	50 ns

Table 1.1: Description of measure setups. In first column there is the gas; second column is the setup name; third column is voltage pulse time width, expressed as percentage of a square trigger 10 µs long; four and fifth columns are target information, where it's used a target; sixth column is used gas flow; seventh column are other informations, i.e. if it's used the conductor ring explained before; eight column is the time step between two different frames.

y axis and it's average luminosity. With barycenter coordinates it's possible to compute their velocity using a finite differance formula (that takes into consideration possible different time steps, see [9]).

Actual dimensions on a frame are found with a calibration with a known target: it is used a plate with 4 holes, diameter of 1.0 ± 0.1 mm at the vertice of a square with an edge lenght of 10.0 ± 0.1 mm, positioned at plasma exit (source is off) and illuminated from behind with a torch. Acquiring a frame of this setup it's possible to extrapolate pixel's distance that corresponds to 10 mm for every square edge, average them, and calculate pixel's width in our frames, resulting a value of $d_{pix} = 0.172 \pm 0.002$ mm.

1.2 Helium flow

We start the presentation of measures with helium, as it is commonly used for medical applications of plasma. Helium it's an element with standard atomic weight of 4.002, 1st ionization energy of 24.587 eV and 2nd ionization energy of 54.418 eV. It's easy to produce helium plasma, when it's ignited it emits radiation with principal wavelenghts in violet and orange ($\lambda = 388.86$ and 587.56 nm), resulting in a purple plume at naked eye. Principal downside of helium gasses it's that they are expensive.

In our experiment we produce helium plasma with pulse frequency $f = 5$ kHz and $\Delta t = 3$, 3.5 and 4 µs, as explained in table 1.1. Delays are setted to take a single frame during every acquisition, for every measure we take 5 frames and average them.

First we present a tipical discharge without target, after is shown how the behavior changes varying parameters and then it's discussed how a target influences bullet propagation.

1.2.1 Plasma bullet description

We use as example bullet the setup D with $\Delta t = 3.5$ µs, i.e. absence of a target and gas flow of 2 L/min.

It's possible to divide the phenomenon that we want to observe in four phases, as presented in figure 1.7: bullet formation, bullet displacement inside the nozzle, bullet expulsion and bullet propagation outside the nozzle, in air. It's important to remember that time values goes from the start of the voltage peak, extrapolated from oscilloscope measures. When the voltage goes over a definite value, we observe a rapid increase in luminosity around the electrode that it's interpreted as plasma formation. From there, in a time of ~ 50 ns the plasma modifies it'shape and becames what we call the bullet: a zone with high luminosity confined in space. The bullet then moves in the exit direction and it's expelled always with a well defined front. In air we see the round shaped bullet propagation, until it reaches a maximum travel distance and then luminosity decreases rapidly, until we see nothing more. In these measure conditions we see again plasma formation in correspondence of the negative tension peak, but it is a rapid process without propagation.

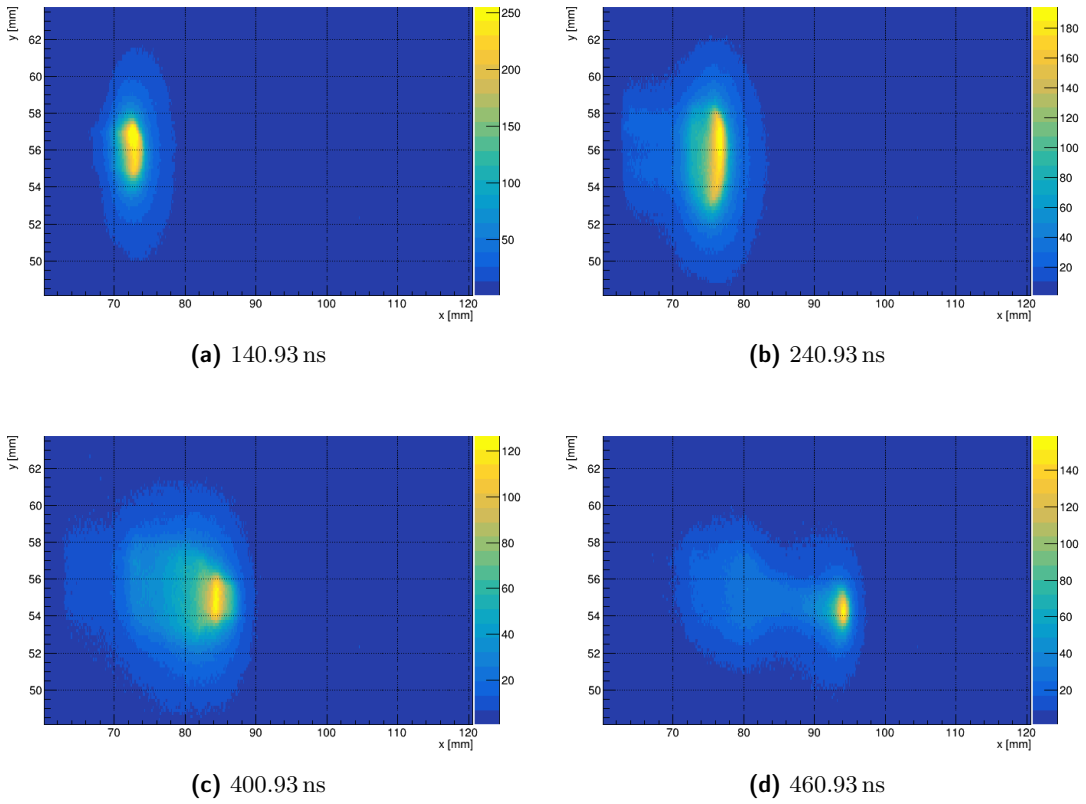

(a) 140.93 ns **(b)** 240.93 ns

(c) 400.93 ns **(d)** 460.93 ns

Figure 1.7: Four phases of plasma dynamics: bullet formation (a), bullet displacement inside the nozzle (b), bullet expulsion (c) and bullet propagation outside the nozzle (d). Time intervals are calculated from the start of the voltage peak.

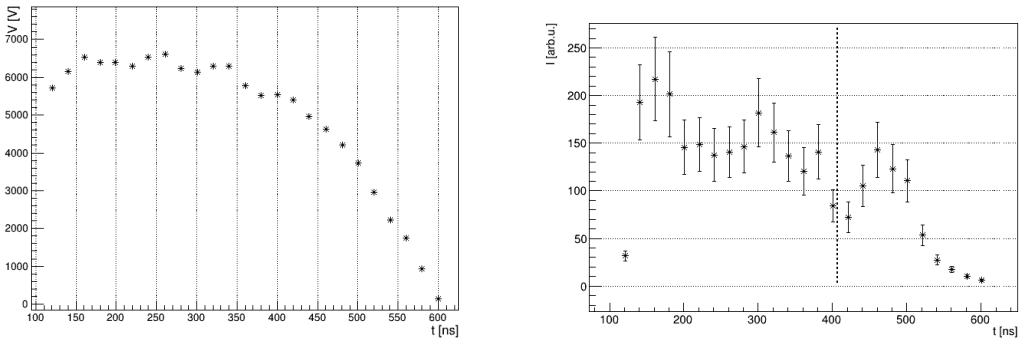

(a) Zoom on voltage waveform.

(b) Mean intensity of plasma bullet.

Figure 1.8: Voltage waveform and intensity of the bullet versus time. Time zero is the start of the voltage peak, ending time is taken as the time where intensity reaches background value. The pointed line in intensity graph indicates the end of the nozzle.

Electrode voltage and bullet intensity The time interval in wich we see the bullet can be defined as where we can see a definite zone with mean luminosity higher then the background. The starting time is given by voltage reaching a certain value, when we see bullet formation, and the bullet expires when it's luminosity decreases.

In figure 1.10 are presented the mean intensity of the plume during the motion and the zoom on the intersted time interval for voltage measure. Plasma formation is observed around 120.93 ns after peak start, at a tension value of 5710.00 ± 285.50 V. As we can see, luminosity is higher during plasma formation around the electrode and it decrease very little during all the propagation, even after the expulsion in air (pointed line on the graph). After a time of 440 ns the bullet luminosity decreases rapidly and it disperses in the air.

Barycenter coordinates and direction The motion of the bullet on observing plane can be extrapolated from it's barycenter coordinates.

In figure **??** there are the two coordinates versus time. Coordinate x, along the axis of the source (of the electrode and the nozzle) is more relevant to observe bullet expulsion. We see as plasma forms around position 73 mm and the nozzle ends at 85 mm, compatible with the distance electrode-nozzle exit described before. After plasma formation we can see bullet displacement in the nozzle with a certain velocity, until it reaches the exit and propagates in the air more rapidly. The bullet travels until it reaches a maximum x, covering a distance of 26.08 ± 0.02 mm from the electrode. It seems that the bullet stops while it's luminosity decreases.

Coordinate y it's relevant to show bullet direction, as we can see, it moves in a space interval of 2 mm. The bullet forms over the electrode, then, when it enlarges to cover all the nozzle diameter, lowers it's barycenter with a constant slope, even after the expulsion. Once the bullet starts to decrease in luminosity, it stops its motion also on the y direction.

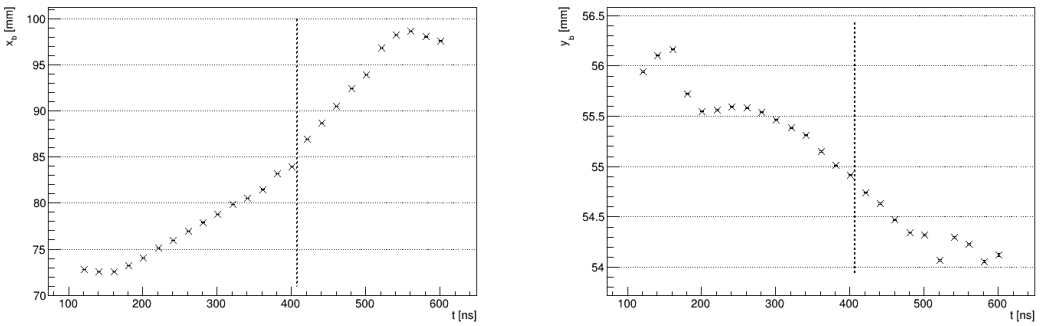

(a) (b)

Figure 1.9: Barycenter coordinates of the bullet. Pointed lines indicate the end of the nozzle.

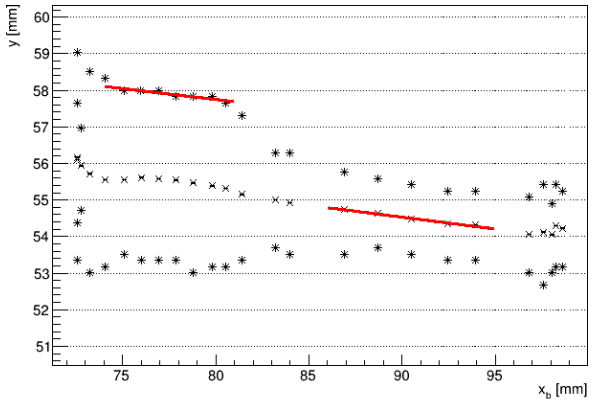

Lowering of the baricenter in the y direction it's explainable by a tilt in the source, that is not perfectly perpendicular to the optical bench, if we consider the entire dimension of the bullet in the y direction, with it's upper and lower limits. In figure **??** are shown y maximum, minimum and baricenter of the bullet, in function of the x brycenter coordinate and can be seen how the entire figure points downward (to the side turning the image). Inside the nozzle we can take y maximum as a value that defines the contour of the nozzle, with a fit as in figure we find a value of $3.39 \pm 0.10°$. Outside the nozzle we find that the barycenter direction is pointed $3.71 \pm 0.04°$ downward, a little higher then the direction of the nozzle. The values are almost compatible with each other, so it seems to suggest that tilting the source it's possible to direct the bullet even after it's propagation in air.

Bullet dimensions Once we define the contour of the bullet, it's simple to take it's dimensions along the two directions.

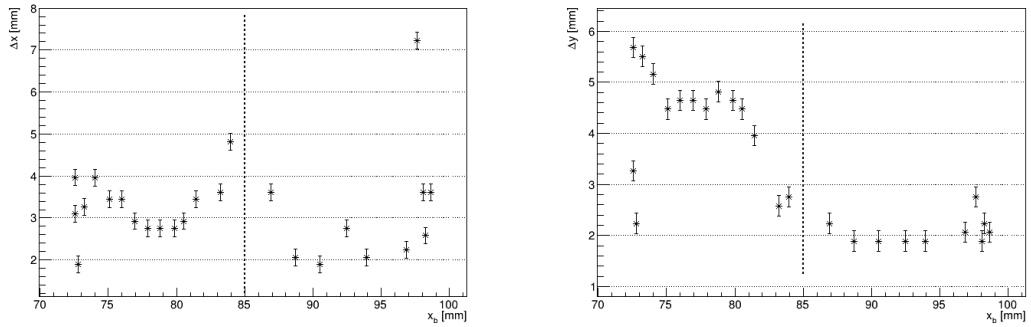

Figure 1.10: Dimensions of the bullet. Pointed lines indicate the end of the nozzle.

In figure **??** are presented width and height of the bullet. In the x direction, the bullet presents constant diameter until it approaches nozzle exit, where it enlarges a little to reach the exit. In the air the bullet mantaines its dimension, with values a little lower then inside the nozzle, but compatible within the error. When it stops it seems to have greater diameter, but the measure loses significance as the bullet fades in the air and it can be confused with the background. In y direction we find a constant value of $4.65 \pm 0.20\,\text{mm}$ during propagation in the nozzle, as expected because the bullet covers all the nozzle area, a little lower then its diameter due to glass refraction effects. Once the nozzle shrinks, the bullet diminish it's diameter and maintains a constant value of $2.07 \pm 0.20\,\text{mm}$ during all the propagation in air, until it stops.

Bullet velocity From barycenter graphs we see as bullet motion has a definite velocity during described phases. Fitting the graph with a line during the displacement phase inside the nozzle, as in figure 1.11, we find that it moves with a speed of $v_{\text{disp}} = 46.48 \pm 0.20\,\text{km/s}$. Once it exits the nozzle it speeds up, until a value of $v_{\text{prop}} = 95.16 \pm 0.60\,\text{km/s}$.

With a 3 point finite differance formula we can estimate it's velocity point by point (excluding the first and the last), finding the values shown in figure 1.11. From those values we can average velocities during the two motion phases, finding compatible mean value respect the linear fit: $v_{\text{disp}} = 48.23 \pm 1.03\,\text{km/s}$ and $v_{\text{prop}} = 95.16 \pm 1.82\,\text{km/s}$.

It's interesting to point out that those velocities are much higher then the average velocity of the neutral gas, that for a flow of $2\,\text{L/min}$ is of $12\,\text{m s}$.

1.2.2 Voltage influence

With an higher Δt we can reach higher voltage peak values (see chapter **??**), so we will have higher electron energies. With more energy we expect that the bullet will reach furter distances, with higher velocity. In figure 1.13 and table 1.3 are presented the results of the analysis.

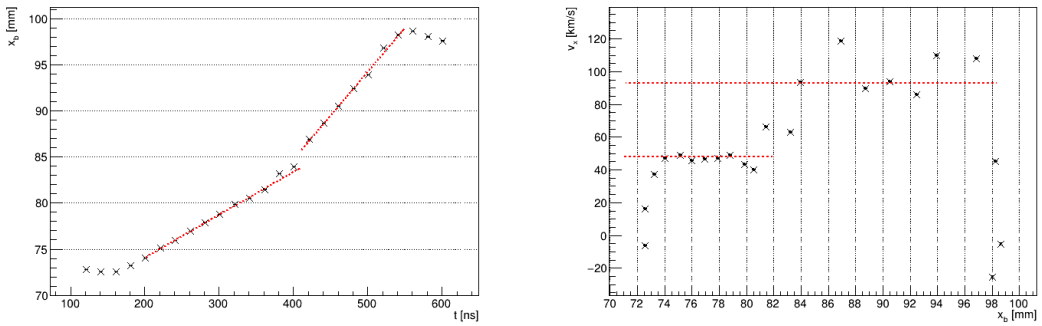

(a) Fit of x barycenter.

(b) Velocities in x direction.

Figure 1.11: Velocity of the bullet in x direction. Pointed lines indicate the end of the nozzle, red lines calculated values during displacement and propagation phases.

The discharge starts always in the same voltage interval, around 5.7 kV. We observe a higher luminosity with higher tensions, but it decreases always in a time interval around 100 ns once it exits the nozzle (figure 1.13 (a)).

The plot for the barycenter coordinates (figure 1.13 (b) - (c)) shows how with higher voltage the bullet reaches further distances (x_{dist} and y_{dist} in table). For the lower voltage peak it seems that the bullet doesn't propagate in air, as it stops right after nozzle exit.

Dimensions of the bullet (figure 1.13 (d) - (e)) are not influenced by voltage value, as we can see they have the exact same behavior, around the same values, for every opening time. A notable differance it's in the y diameter inside the nozzle, where for higher tension we have a slightly larger value. As mentioned before here we have refraction effects due to the glass nozzle, different for those measures due to the higher luminosity.

Velocity values (figure 1.13 (f)) show how the bullet behavior is solid during the propagation inside the nozzle and becames more erratic once it exits. As mentioned before, for the lowest opening time we have lower velocities and a rapid drop after contact with air, in this configuration it's not possible to find a propagation velocity. For higher opening times we find the same behavior, with a proportionality between peak voltage value and velocities: if before we found a stable motion with $v_{\text{prop}} = 92.93 \pm 0.06$ km/s, with higher tension it reaches $v_{\text{prop}} = 149.47 \pm 0.09$ km/s.

1.2.3 Flow influence

As said before, neutral gas velocity is very little in comparision of the ionization front velocity of the bullet, we expect that changes in the gas flow will have an effect on the quantity of helium present in the nozzle more then on the energy of the atoms and electrons. We try four different flows with the same peak voltage, in figure 1.13 and table 1.3 are presented the results of the analysis.

Also for this parameter, the discharge starts always in the same voltage interval, around 5.7 kV. For gas flows of 1 and 2 L/min bullet luminosity decreases in a time

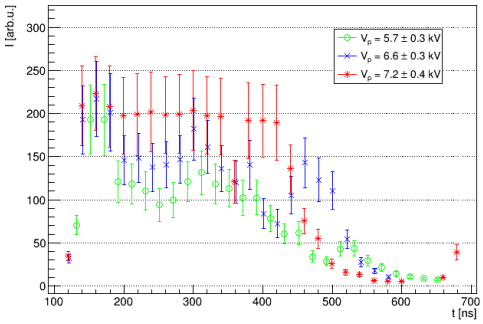

(a) Mean luminosity.

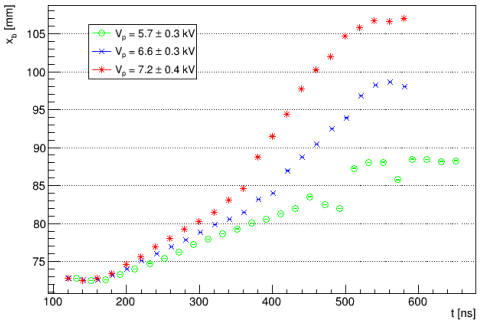

(b) x barycenter.

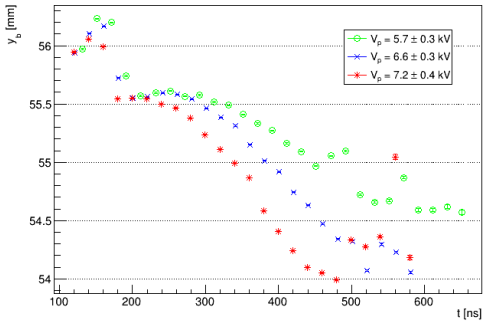

(c) y barycenter.

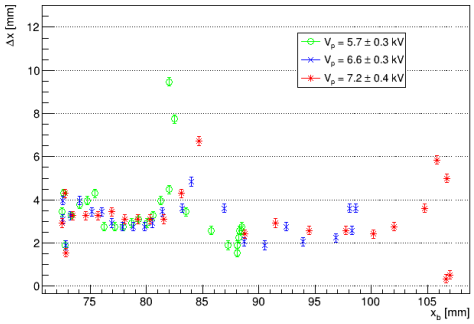

(d) x diameter.

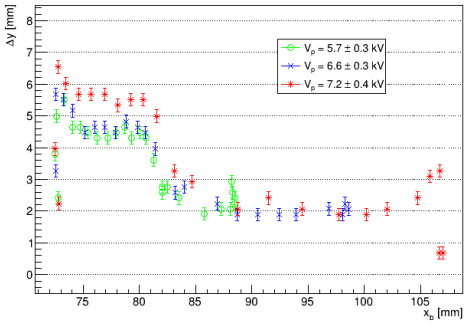

(e) y diameter.

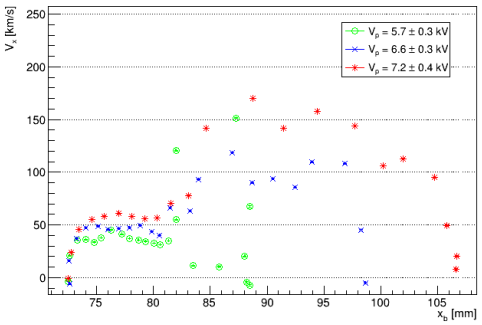

(f) x velocity.

Figure 1.12: Results of the analysis for setup d (helium flow of 2 L/min without target), with different peak voltage values.

V_p [kV]	V_0 [kV]	x_{dist} [mm]	y_{dist} [mm]	v_{disp} [km/s]	v_{prop} [km/s]
5.66 ± 0.30	5.55 ± 0.28	15.99 ± 0.01	1.66 ± 0.02	37.72 ± 0.04	-
6.59 ± 0.33	5.71 ± 0.29	26.08 ± 0.02	1.92 ± 0.04	46.48 ± 0.02	95.16 ± 0.06
7.22 ± 0.36	6.01 ± 0.30	34.55 ± 0.05	2.07 ± 0.01	59.80 ± 0.03	149.47 ± 0.09

Table 1.2: Result of the analysis with different voltage peak values for the pulse. V_p is the peak value for the pulse, V_0 bullet formation tension, x_{dist} and y_{dist} are the highest distances reached by the bullet from electrode position, v_{disp} is the velocity in x direction reached inside the nozzle, v_{prop} is the velocity of propagation in air in x direction.

interval around 100 ns once it exits the nozzle, for higher flows it has a luminosity clearly stronger then background for a longer time interval, around 200 ns (figure **??** (a)).

From the barycenter coordinates (figure 1.13 (b) - (c)) we see as more gas flow seems to be correlated with lower mobility of the bullet: we have shorter distances with higher flows. For maximum tried flow, even if bullet luminosity is more then the background, the bullet travels a very little distance from the exit of the nozzle and it's barycenter remains almost fixed in space.

Dimensions of the bullet (figure 1.13 (d) - (e)) are not very influenced by gas flow, but we can see little inverse proportionality. For stronger flows we have always littler diameters inside the nozzle, in both directions.

Velocities shows how the bullet behavior changes also inside the nozzle varying gas flow (figure 1.13 (f)). With little flow, we find a costant displacement velocity in the nozzle, while with more flow the bullet slows down when moving (as shown in [5]), with a decrease in velocity of 7.58 ± 0.04 km/s/mm. Once the bullet exits the nozzle, we see how it almost stops when there is high flow, while it shows the same behavior if flow is under 3 L/min and it has maximum velocity for the lowest gas flow, maintaining it for longer time.

Can be concluded that with higher flow we have bullet with longer lifetime and littler mobility, reaching lesser distances with lesser velocity.

1.2.4 Insulator target

Plasma produced with this source will be applied on biological tissues, so it's fundamental to know how bullet behavior changes with different targets.

An insulator target is not expected to affect the behavior until the bullet reaches it. An intersting effect is seen after the impact of the bullet with the target, as in figure 1.14, where the plasma seems to deposit charge on the insulator in a circular shape.

In figure 1.15 we can see barycenter's x-coordinate of the bullet and its diameter. While for the lowest tension value we see that the bullet stops before it reaches the target, for the other two sets it clearly stops at the target position. Distance values are comparable with those without target (figure 1.13), a little higher for medium tension

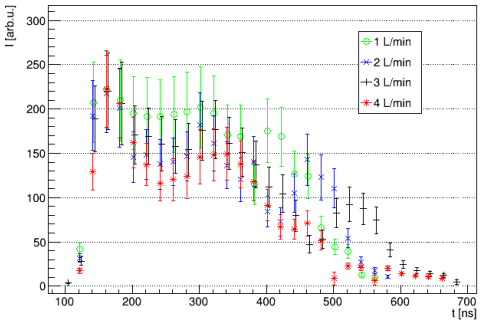

(a) Mean luminosity.

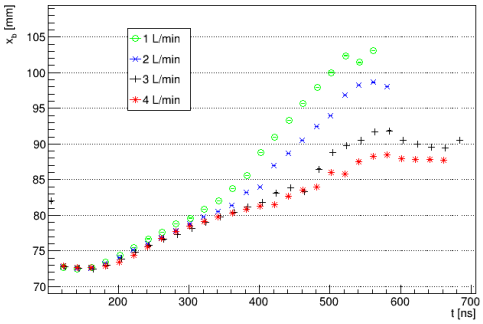

(b) x barycenter.

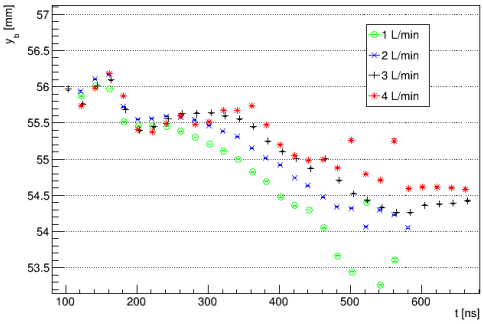

(c) y barycenter.

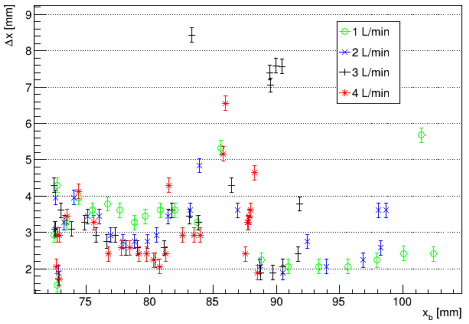

(d) x diameter.

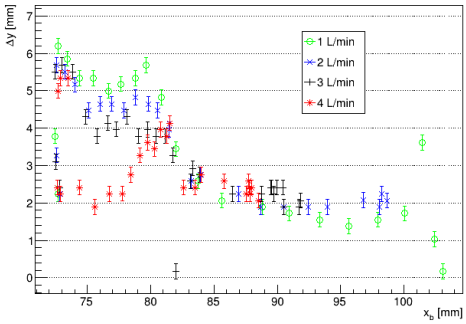

(e) y diameter.

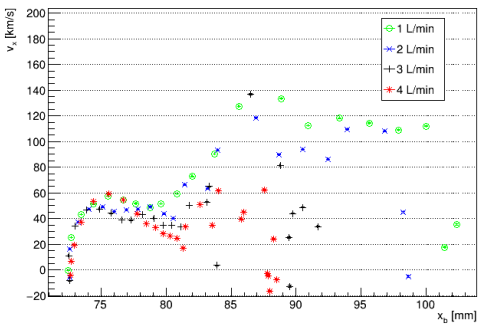

(f) x velocity.

Figure 1.13: Results of the analysis for different gas flow (opening time of 3.5 µs without target).

Flow [L/min]	V_0 [kV]	x_{dist} [mm]	y_{dist} [mm]	v_{disp} [km/s]	v_{prop} [km/s]
1	5.87 ± 0.08	30.65 ± 0.03	2.75 ± 0.01	54.33 ± 0.10	113.97 ± 0.09
2	5.71 ± 0.29	26.08 ± 0.02	1.92 ± 0.04	46.48 ± 0.02	95.16 ± 0.06
3	5.41 ± 0.27	19.38 ± 0.01	1.84 ± 0.01	39.88 ± 0.04	40.96 ± 0.10
4	5.90 ± 0.12	22.80 ± 0.03	2.30 ± 0.01	58.89 ± 0.14	61.94 ± 0.44

Table 1.3: Result of the analysis with different gas flows. V_0 the bullet formation tension, x_{dist} and y_{dist} are the highest distances reached by the bullet from electrode position, v_{disp} is the velocity in x direction reached inside the nozzle, v_{prop} is the velocity of propagation in air in x direction.

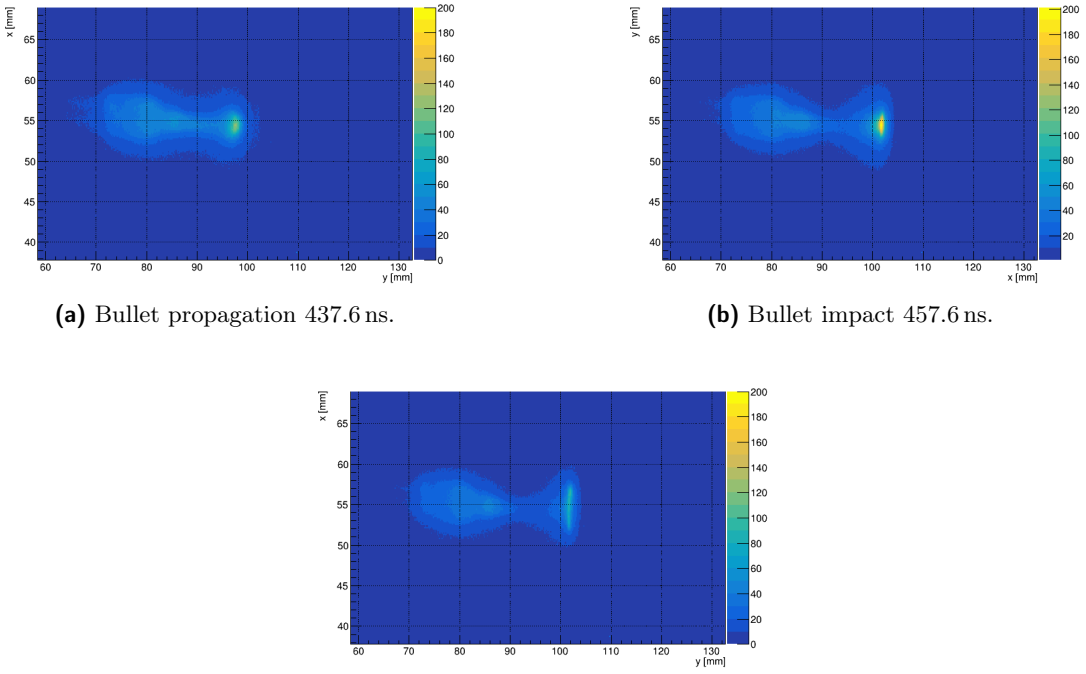

(a) Bullet propagation 437.6 ns.

(b) Bullet impact 457.6 ns.

(c) Charge deposition 577.6 ns.

Figure 1.14: Impact and charge deposition on an insulator target.

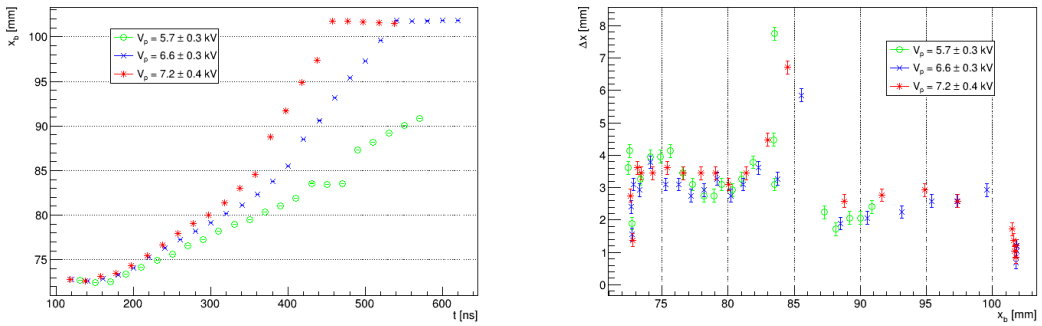

(a) Barycenter position. **(b)** Bullet diameter.

Figure 1.15: Barycenter motion and diameter in x direction, for different voltage peak values.

value, as the bullet instead of stopping at a position before it (as it does whitout target) collide with the target. Bullet width is exactly the same with or without target during it's propagation. We can see changes only when it impacts on the target and shrinks rapidly. Displacement velocities inside the nozzle and propagation velocities in air are of the same order of values without target, as we can see in figure **??**. We find higher v_{prop} only for medium tension value, where it reaches $118.98 \pm 0.07\,\text{km/s}$, due to the rapid collision with the target instead of slowing down and stopping.

Charge deposition Once the bullet reaches the target we can see how the glowing region enlarges on its surface from the plot of y diameter, as in figure 1.16. To evaluate the expansion diameter and velocity, we can plot the differance between y limit and y barycenter once the bullet reaches the target. In figure 1.16 we can see that the diameter of the maximum expansion is little higher for larger tension value, as well as it's expansion velocity: for opening time of $3.5\,\mu\text{s}$ we find a diameter of $6.54 \pm 0.04\,\text{mm}$ and an expansion velocity of $31.36 \pm 0.25\,\text{km/s}$, while for $4.0\,\mu\text{s}$ we find $7.40 \pm 0.02\,\text{mm}$ and $64.04 \pm 0.39\,\text{km/s}$. It is an expected result as the bullet have more energy with an higher peak value, the velocity along x is larger and we have also higher expansion velocity.

1.2.5 Distant conductive target

A conductive target is expected to affect bullet behavior as it reachs its proximity, as there are free charges on the surface. If with an insulator we see charge deposition, with a conductor we see a rapid backstream (with a motion inverse to that of the bullet) with great luminosity when the bullet impacts on it, as in figure 1.17.

Bullet dynamics Considering only the bullet, separated from the backstream, first thing to note with this target, is how all the system is more reactive to tension values:

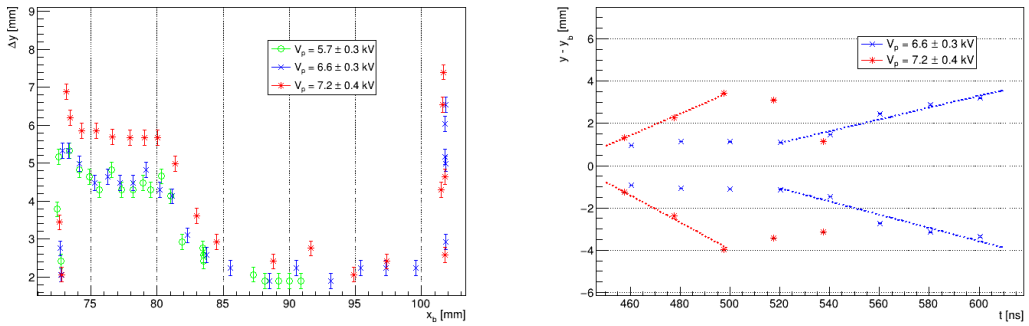

(a) Bullet diameter.

(b) Bullet expansion in time.

Figure 1.16: Bullet expansion in the y direction. We see the absolute value for the diameter for all barycenter positions (a) and a zoom on the expansion for times after it reaches the target (b), where y contour values are calculated as differance with the barycenter y coordinate. Linear fits show how much the diameter enlarges in time.

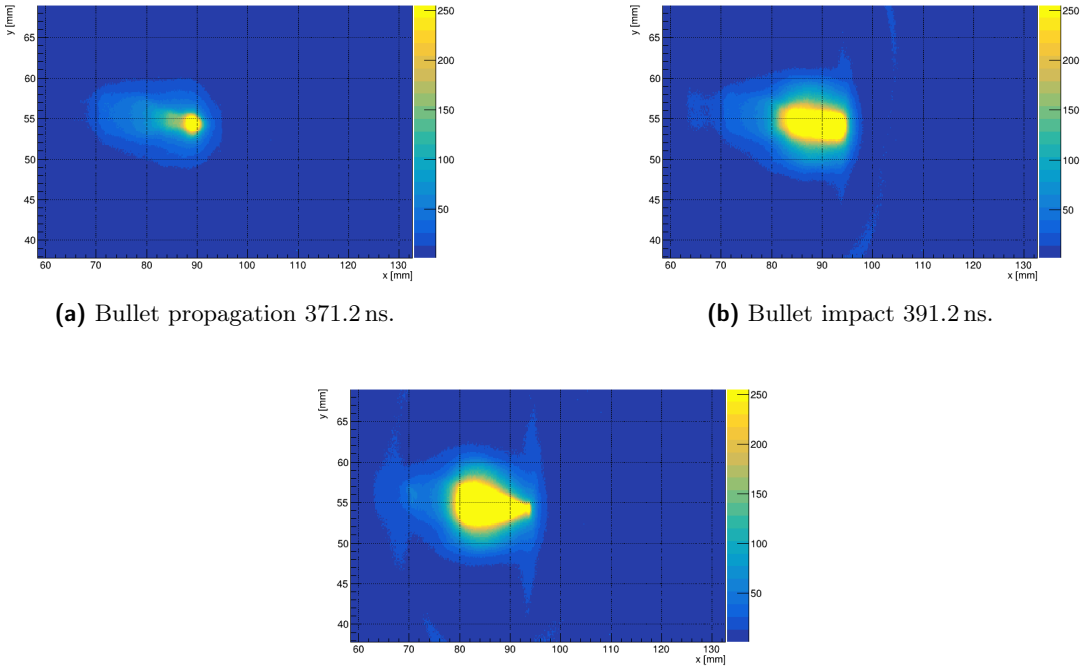

(a) Bullet propagation 371.2 ns.

(b) Bullet impact 391.2 ns.

(c) Backstream 411.2 ns.

Figure 1.17: Impact and backstream with a copper target.

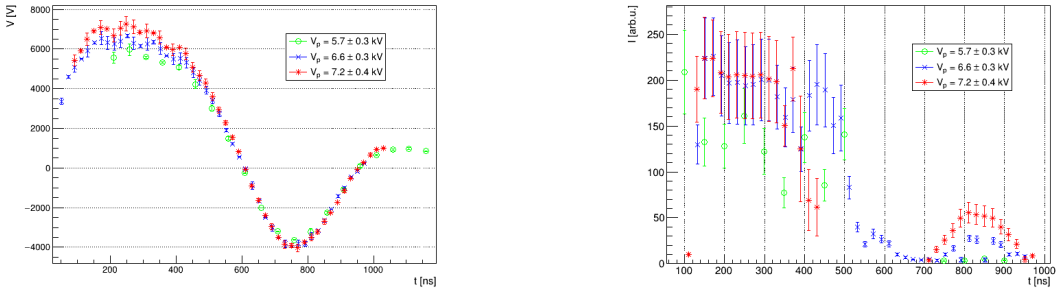

(a) Voltage waveforms.

(b) Bullet luminosity.

Figure 1.18: Voltage applied to the elctrode and bullet luminosity for different measure sets. Note the second luminosity peak in correspondence of the negative voltage peak.

as we can see in figure 1.18, we find that plasma bullet luminosity is enanched in correspondence of the second tension peak (negative), even if it doesn't move from the target as shown in figure 1.19 (a). Thanks to this second peak, bullet lifetime is longer, it shows luminosity even after 900 ns from the start.

Barycenter motion shows also some peculiarities: even with low tension the bullet reaches the target, showing larger propagation velocity then with other configurations. It's diameter doesn't shows different behavior, it stays constant until nozzle exit and remains constant until it reaches the target and shrinks to a point. As said before, velocities of propagation in air are generally larger then whitout target, they arrives from 112.04 ± 0.05 km/s for low voltage peak to 160.55 ± 0.09 km/s for high voltage peak.

Current measure Thanks to the conductive target, we can measure current intensity flowing in it due to charge transported by bullets, and, more intersting, the relation between impact time and when it's measured peak current. Current intensity it's shown in figure 1.20, we can see a positive peak, more influenced by tension peak value, and a negative peak in correspondence of the negative tension peak and of the second luminosity peak for the bullet.

In the graphs we can distinguish a starting time for the peak current, and a time where it reaches it's maximum value. Even if it's difficult to establish precisely the starting time, we can see as both of them are larger for lower tension values, we have lower and slower current intensity when bullets have less energy. To study the relation between those values, we extrapolate relevant times and the bullet distance from the target when we start to see current, presented in table **??**. From the values we can see that we begin to measure current before the bullet barycenter reaches the target, and even maximum current is measured before the impact time of the bullet for medium and high tension value. We can estimate a distance of interaction as the differance between bullet barycenter position and target position. This distance becames larger when we set an higher voltage for the pulse, when the bullet velocity is higher.

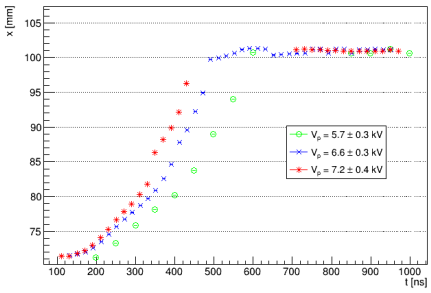

(a) Barycenter.

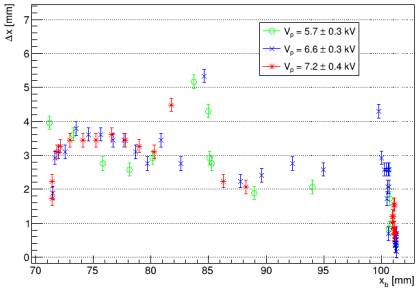

(b) Diameter.

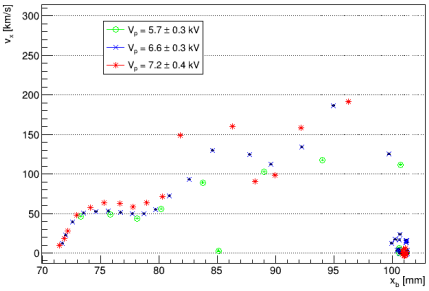

(c) Velocity.

Figure 1.19: Bullet barycenter coordinate, diameter and velocity along x direction, with copper target. When the bullet reaches the target, it shrinks and stops.

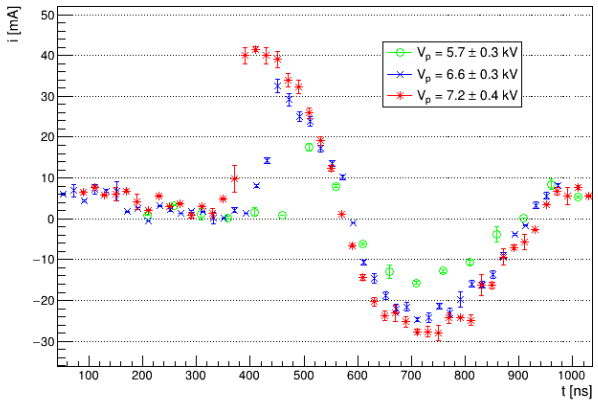

Figure 1.20: Current intensity measured in set A, with different voltage peak values.

V_p [kV]	i_p [mA]	$t_{0,i}$ [ns]	$t_{p,i}$ [ns]	t_{imp} [ns]	$x_{\text{target}} - x(t_{0,i})$ [mm]
5.7 ± 0.3	17.56 ± 0.88	459.1 ± 15.0	509.2 ± 15.0	499.1 ± 15.0	7.20 ± 0.01
6.6 ± 0.3	32.63 ± 1.63	391.6 ± 15.0	451.6 ± 15.0	511.6 ± 15.0	9.22 ± 0.01
7.2 ± 0.4	41.50 ± 0.62	350.3 ± 15.0	410.3 ± 15.0	450.3 ± 15.0	15.18 ± 0.02

Table 1.4: Values extrapolated from current measure and bullet barycenter motion. V_p is the voltage peak for the pulse, i_p is the current peak value, $t_{0,i}$ is the starting time for the current value, $t_{p,i}$ is the time of the peak value, t_{imp} is the time of the impact of bullet on target, $x_{\text{target}} - x(t_{0,i})$ is the distance between bullet position when we start to measure current and target position.

Current measure can be explained if the bullet motion is associated with charge motion: as the bullet travels towards the target, charges with highest speed reach the target before the barycenter and we begin to measure current before it reaches the target. When the bullet has higher energy, charges have more speed, arrive before to the target and more of them interacts with it, so we will have an higher peak, positioned before in time.

Backstream Dynamics of the backstream from the target is difficult to analyze as it's a rapid phenomenon with too high luminosity. We see that the frames right after the impact of the bullet on target, present another zone with high luminosity right after nozzle exit. This other glow has stable position and diameter, as can be seen in figure 1.21, with a slow tendency to shift towards the target when voltage is positive and towards the electrode when it's negative. The phenomenon can be explained as a very rapid charge stream from the target to the electrode, that stops when meets the nozzle, but to study it are necessary other specific measures with lower velocities (for example increasing gas flow, see before) or more time resolution.

1.3 Neon flow

1.4 Argon flow

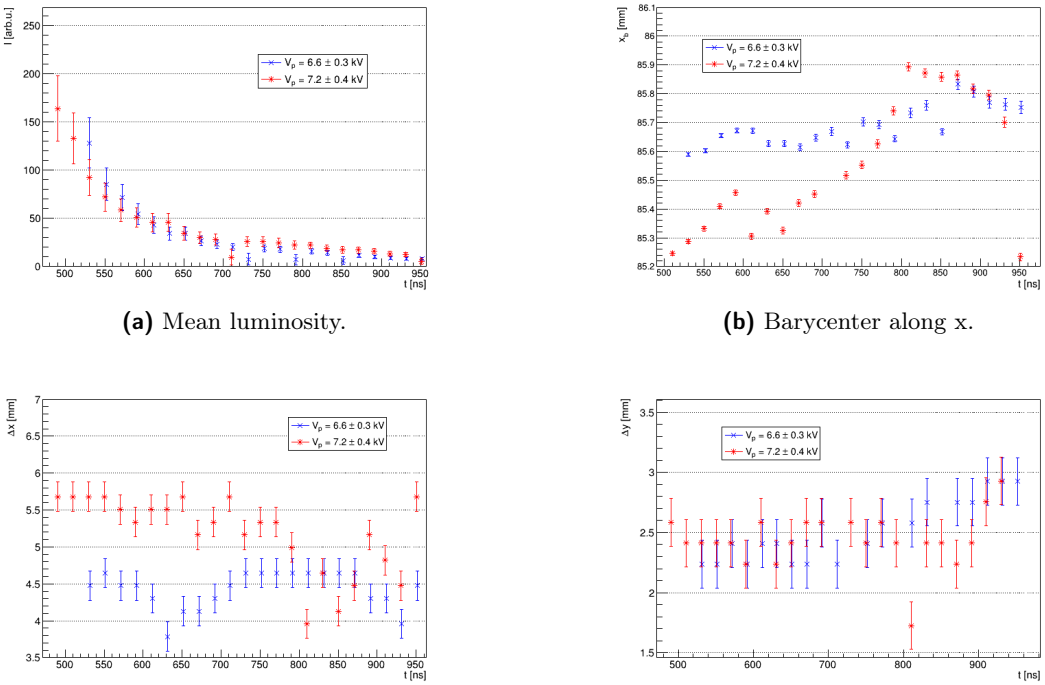

(a) Mean luminosity.

(b) Barycenter along x.

(c) Diameter along x.

(d) Diameter along y.

Figure 1.21: Backstream features in time.

Bibliography

[1] URL: https://www.ptgrey.com/Content/Images/uploaded/Flea.pdf.

[2] URL: http://netpbm.sourceforge.net/doc/pgm.html.

[3] D Breden, K Miki, and L L Raja. "Self-consistent two-dimensional modeling of cold atmospheric-pressure plasma jets/bullets". In: *Plasma Sources Science and Technology* 21.3 (2012), p. 034011. DOI: 10.1088/0963-0252/21/3/034011. URL: https://doi.org/10.1088%2F0963-0252%2F21%2F3%2F034011.

[4] R. Brun. *ROOT documentation for TH2 class*. URL: https://root.cern.ch/doc/master/classTH2.html.

[5] Julien Jarrige, Mounir Laroussi, and Erdinc Karakas. "Formation and dynamics of plasma bullets in a non-thermal plasma jet: influence of the high-voltage parameters on the plume characteristics". In: *Plasma Sources Science and Technology* 19.6 (2010), p. 065005. DOI: 10.1088/0963-0252/19/6/065005. URL: https://doi.org/10.1088%2F0963-0252%2F19%2F6%2F065005.

[6] N Mericam-Bourdet et al. "Experimental investigations of plasma bullets". In: *Journal of Physics D: Applied Physics* 42.5 (2009), p. 055207. DOI: 10.1088/0022-3727/42/5/055207. URL: https://doi.org/10.1088%2F0022-3727%2F42%2F5%2F055207.

[7] Seth A. Norberg, Eric Johnsen, and Mark J. Kushner. "Helium atmospheric pressure plasma jets touching dielectric and metal surfaces". In: *Journal of Applied Physics* 118.1 (2015), p. 013301. DOI: 10.1063/1.4923345.

[8] Eric Robert et al. "Experimental Study of a Compact Nanosecond Plasma Gun". In: *Plasma Processes and Polymers* 6.12 (2009), pp. 795–802. DOI: 10.1002/ppap.200900078.

[9] ashok kumar Singh and Beer Bhadauria. "Finite Difference Formulae for Unequal Sub-Intervals Using Lagrange's Interpolation Formula". In: *Journal of Math. Analysis* 3 (Jan. 2009), pp. 815–827.

[10] Wen Yan and Demetre J. Economou. "Simulation of a non-equilibrium helium plasma bullet emerging into oxygen at high pressure (250–760Torr) and interacting with a substrate". In: *Journal of Applied Physics* 120.12 (2016), p. 123304. DOI: 10.1063/1.4963115.